

# Optimal control of high-order harmonics for the generation of an isolated ultrashort attosecond pulse with two-color midinfrared laser fields

Yi Chou,<sup>1,\*</sup> Peng-Cheng Li,<sup>1,2,†</sup> Tak-San Ho,<sup>3,‡</sup> and Shih-I Chu<sup>1,4,§</sup>

<sup>1</sup>*Center for Quantum Science and Engineering, Department of Physics, and Center for Advanced Study in Theoretical Sciences, National Taiwan University, Taipei 10617, Taiwan*

<sup>2</sup>*College of Physics and Electronic Engineering, Northwest Normal University, Lanzhou 730070, China*

<sup>3</sup>*Department of Chemistry, Princeton University, Princeton, New Jersey 08544, USA*

<sup>4</sup>*Department of Chemistry, University of Kansas, Lawrence, Kansas 66045, USA*

(Received 22 March 2015; published 12 June 2015)

We present an efficient high-order-harmonic optimal control scheme for the generation of the ultrabroad supercontinuum spectrum and an isolated ultrashort attosecond pulse in gases with a two-color mid-IR laser field. The optimal control scheme is implemented using a derivative-free unconstrained optimization algorithm called NEWUOA (NEW Unconstrained Optimization Algorithm). For illustration, the high-order-harmonic generation (HHG) of a hydrogen atom is considered for optimization. It is shown that optimally shaped laser waveforms can greatly enhance and extend the HHG plateau and efficiently generate an isolated ultrashort attosecond pulse. Moreover, by performing accurate semiclassical simulations and a detailed wavelet time-frequency analysis, we found that the optimized supercontinuum harmonics corresponding to long-trajectory electrons are responsible for an isolated ultrashort 21-as pulse.

DOI: [10.1103/PhysRevA.91.063408](https://doi.org/10.1103/PhysRevA.91.063408)

PACS number(s): 32.80.Qk, 32.70.Jz, 42.50.Hz

## I. INTRODUCTION

In the past two decades, the advent of attosecond laser pulses has led to real-time observation of the dynamics in atomic and molecular processes. In particular, the generation of isolated ultrashort attosecond pulses has received much attention in ultrafast science. A promising way to produce isolated ultrashort pulses is to achieve the superposition of a broadband supercontinuum in high-order-harmonic generation (HHG) [1,2]. Recently, a 67-as pulse, the shortest attosecond pulse at present, has been produced in the laboratory [3].

The HHG spectrum is characterized by a rapid drop at low orders, followed by a typically broad plateau where all the harmonics have a similar strength, and terminated with a sharp cutoff at the end of plateau, beyond which no further harmonic emission is observed. This can be understood by a semiclassical three-step model [4]. It is also demonstrated that for a single-atom response, the cutoff is located around the energy equal to  $I_p + 3.17U_p$ , where  $I_p$  is the atomic ionization potential and  $U_p$  is the laser ponderomotive potential. On the basis of the three-step model, the electron first tunnels through the modified potential barrier jointly created by the Coulomb potential and the interaction with the laser field, then accelerates and acquires additional kinetic energy, and, finally, after recolliding and being recaptured by the parent ion, emits high-energy photons.

The optimal control theory (OCT) [5,6] has been extensively applied in controlling atomic and molecular processes [7]. For example, the application of the OCT in strong-field ultrafast atomic phenomena has produced properly shaped laser pulses for enhancing and suppressing ionization [8–10].

In particular, it has been found that the optimized control field not only can effectively suppress the ionization but also can result in an increase in the HHG yield and the absence of clear cutoffs [10]. Recently, different theoretical schemes have been proposed [11–14] for optimizing two-color laser pulses to extend the HHG cutoff in supercontinuum regimes for generation of attosecond pulses.

In the present work we extend the OCT to generate an isolated ultrashort attosecond laser pulse with an optimized two-color midinfrared laser pulse to extend the HHG cutoff and enhance the HHG near the cutoff region. The underlying time-dependent Schrödinger equation (TDSE) is solved using the time-dependent generalized pseudospectral method (TDGPS) [15]. The time-frequency characteristics of the attosecond pulses are analyzed by performing the wavelet transform of the induced dipole. It is shown that a 21-as pulse can be attained via the superposition of an ultrabroad supercontinuum in the hydrogen atom HHG produced by optimizing a two-color mid-IR laser pulse.

The remainder of the paper is organized as follows. Section II outlines the theoretical method for computing the HHG spectrum, performing time-frequency analysis, and generating isolated ultrashort attosecond pulses. Section III describes the OCT iterative scheme based on NEWUOA (NEW Unconstrained Optimization Algorithm) [16], a derivative-free algorithm. Section IV presents the simulation results and discussions. Finally, Sec. V gives a summary as well as some perspectives of this work.

## II. THEORETICAL METHOD

We consider a hydrogen atom in the presence of an intense laser field; the governing TDSE (in atomic units) can be written as

$$i \frac{\partial \psi(\mathbf{r}, t)}{\partial t} = \hat{H}(\mathbf{r}, t) \psi(\mathbf{r}, t) = [\hat{H}_0(\mathbf{r}) + \hat{V}(\mathbf{r}, t)] \psi(\mathbf{r}, t), \quad (1)$$

\*r00222008@ntu.edu.tw

†lipc@nwnu.edu.cn

‡tsho@princeton.edu

§sichu@ku.edu

where the unperturbed Hamiltonian for the hydrogen atom takes on the form

$$\hat{H}_0(\mathbf{r}) = -\frac{1}{2}\nabla^2 - \frac{1}{r} \quad (2)$$

and the atom-field interaction in the electric dipole approximation is given as

$$\hat{V}(\mathbf{r}, t) = -\mathbf{E}(t) \cdot \mathbf{r} = -E(t)\hat{\mathbf{z}}, \quad (3)$$

where the laser field  $\mathbf{E}(t) = E(t)\hat{\mathbf{z}}$  is linearly polarized in the  $z$  direction. Equation (1) is solved accurately and efficiently with the TDGPS method in the spherical coordinates. This numerical scheme comprises two significant components: (i) The GPS technique allows the radial coordinates to be optimally discretized in a nonuniform radial grid. With only a modest number of grid points, the discretization is characterized by denser grids near the nuclear origin and sparser grids for larger distances. (ii) The second-order split-operator technique in the energy representation permits elimination of undesirable fast-oscillating high-energy components and thus leads to efficient and accurate time propagation of the wave function according to the relation

$$\begin{aligned} \psi(\mathbf{r}, t + \Delta t) &\simeq \exp\left(-i\hat{H}_0\frac{\Delta t}{2}\right)\exp\left[-i\hat{V}\left(\mathbf{r}, \theta, t + \frac{\Delta t}{2}\right)\Delta t\right] \\ &\times \exp\left(-i\hat{H}_0\frac{\Delta t}{2}\right)\psi(\mathbf{r}, t) + O(\Delta t^3). \end{aligned} \quad (4)$$

Once the corresponding time-dependent wave function is obtained via Eq. (4), the expectation value of the induced dipole moment in the length and acceleration forms can be calculated, respectively, from the relations

$$d_L(t) = \langle \psi(\mathbf{r}, t) | z | \psi(\mathbf{r}, t) \rangle, \quad (5a)$$

$$\begin{aligned} d_A(t) &= \frac{\partial^2}{\partial t^2} \langle \psi(\mathbf{r}, t) | z | \psi(\mathbf{r}, t) \rangle \\ &= \langle \psi(\mathbf{r}, t) | -\frac{z}{r^3} + E(t) | \psi(\mathbf{r}, t) \rangle. \end{aligned} \quad (5b)$$

The HHG power spectra in the length and acceleration forms can be computed, respectively, by the relations

$$P_L(\omega) = \left| \frac{1}{t_f - t_i} \int_{t_i}^{t_f} d_L(t) \exp(-i\omega t) dt \right|^2, \quad (6a)$$

$$P_A(\omega) = \left| \frac{1}{t_f - t_i} \frac{1}{\omega^2} \int_{t_i}^{t_f} d_A(t) \exp(-i\omega t) dt \right|^2, \quad (6b)$$

where  $t_i$  and  $t_f$  are the instants that the control pulse is turned on and off, respectively.

Moreover, a time-frequency analysis via the wavelet transform can be carried out for the induced dipole acceleration  $d_A(t)$  using the relation [2]

$$A(t, \omega) = \int d_A(t) \sqrt{\omega} W[\omega(t' - t)] dt, \quad (7)$$

where the Morlet mother wavelet  $W(t' - t)$  for the harmonic emission is given as

$$W(x) = \frac{1}{\sqrt{\tau_0}} \exp(ix) \exp\left(\frac{-x^2}{2\tau_0^2}\right). \quad (8)$$

Finally, an attosecond pulse can be obtained by superposing different harmonics over a finite-frequency window  $[\omega_i, \omega_f]$ , i.e.,

$$I(t) = \left| \int_{\omega_i}^{\omega_f} D_A(\omega) \exp(i\omega t) d\omega \right|, \quad (9)$$

where  $D_A(\omega) = \int d_A \exp(-i\omega t) dt$ . Here, the values of  $\omega_i$  and  $\omega_f$  have been calculated by trial and error in order to provide the shortest attosecond pulse.

### III. THE NEWUOA-BASED DERIVATIVE-FREE OCT METHOD

The two-color mid-IR laser field that is to be optimally shaped using the derivative-free NEWUOA is given as

$$\begin{aligned} E(t) &= A_1 f_1(t - \tau) \cos[\omega_1(t - \tau)] \\ &+ A_2 f_2(t) \cos(\omega_2 t + \phi), \end{aligned} \quad (10)$$

where  $A_1$  and  $A_2$ ,  $f_1(t)$  and  $f_2(t - \tau)$ , and  $\omega_1$  and  $\omega_2$  are, respectively, amplitudes, Gaussian envelopes, and frequencies of the two constituent pulses;  $\tau$  is the time delay between the two pulses; and  $\phi$  is the carrier-envelope phase (CEP) of the second pulse. In this study, a derivative-free OCT scheme is applied to find a set of optimal control parameters  $\tau$ ,  $\phi$ , and  $A = A_1 + A_2$  (while keeping the ratio  $A_1/A_2$  fixed throughout the calculations) to enhance the HHG and extend the cutoff simultaneously. In this study, the optimization is performed via the maximization of the merit function

$$J[\tau, \phi, A] = \int_{\omega_L}^{\omega_H} \log_{10} P_A(\omega) d\omega, \quad (11)$$

where  $\omega_L$  and  $\omega_H$  are, respectively, the lowest and highest frequencies of the frequency window designated for producing the desired ultrashort attosecond pulse. The merit function  $J$  is maximized with respect to the parameters  $\tau$ ,  $\phi$ , and  $A$  using an efficient and robust derivative-free algorithm called NEWUOA [16], which is a trust-region method based on a local quadratic model. In each NEWUOA-based OCT iteration, a quadratic model is constructed for the merit function  $J[\tau, \phi, A]$  [Eq. (11)] and is minimized to find a new set of control parameters  $x = (\tau, \phi, A)$  for the next iteration. Specifically, after choosing judiciously at the start (i) an initial set of control parameters  $x_0 = (\tau_0, \phi_0, A_0)$ , (ii) the number and the set of interpolation points, and (iii) the starting and ending trust-region radii  $\rho_0$  and  $\rho_{\text{end}}$ , the following three steps at each iteration, here the  $k$ th one, are taken in the NEWUOA-based OCT scheme: (1) constructing the quadratic model of the merit function  $J$  as  $m_k(x_k + s) = d_k + s^T g_k + \frac{1}{2} s^T G_k s$ , where  $d_k$ ,  $g_k$ , and  $G_k$  are determined by the interpolation conditions ( $k = 0$  for kicking off the first iteration); (2) searching for the minimum in the quadratic trust region, e.g.,  $\tilde{s} = \text{argmin } m_k(x_k + s)$  subject to  $|s| \leq \Delta$ ; and (3) updating the trust-region radius  $\rho_k$ , the interpolation set, and the quadratic model. These steps are

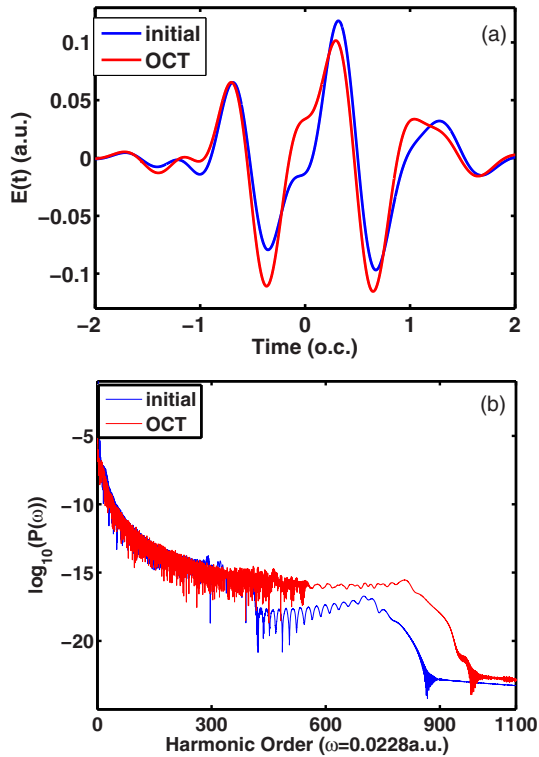


FIG. 1. (Color online) (a) The initial laser field [blue (dark gray) line] and the optimized laser field [red (light gray) line]. (b) The corresponding HHG power spectra in acceleration form.

repeated until the convergence criterion is met, i.e., when  $\rho_k = \rho_{\text{end}}$ .

#### IV. RESULTS AND DISCUSSION

To perform the NEWUOA-based OCT calculations, we consider three control parameters: the CEP  $\phi$ , the time delay  $\tau$ , and the total field amplitude  $A$ . All other parameters of the two-color mid-IR laser fields (including the amplitude ratio  $A_1/A_2$ ) are kept fixed throughout. Specifically, we have chosen the following number: the amplitude ratio  $A_1/A_2 = 2.237$ , the frequency of the primary pulse  $\omega_1 = 0.0228$  a.u. (2000 nm), the frequency of the secondary pulse  $\omega_2 = 0.043$  a.u. (1064 nm), the pulse duration  $t_f - t_i = 8$  optical cycles (o.c.; here,  $t_i = -4$  o.c.,  $t_f = 4$  o.c., and 1 o.c. =  $2\pi/\omega_1$ ), and the FWHMs of both Gaussian pulses = 8 fs = 1.2 o.c. Here, we note that a recent study [14] demonstrated that a right-shifted laser pulse whose peak occurs later than half the laser-operation time may produce a broader HHG plateau than a center-enhanced laser pulse whose peak occurs at half the laser-operation time and a left-shifted pulse whose peak occurs earlier than half the laser-operation time. For that reason, we chose a right-shifted laser pulse as the initial guess. The initial pulse [blue (dark gray) line] and the optimized pulse [red (light gray) line] are presented in Fig. 1(a), corresponding to the parameters  $A_1 = 0.0962$  a.u. ( $I_1 = 3.2 \times 10^{14}$  W/cm<sup>2</sup>),  $A_2 = 0.0430$  a.u. ( $I_2 = 6.5 \times 10^{13}$  W/cm<sup>2</sup>),  $\phi = 0.6\pi$ , and  $\tau = 0.25T_1$  ( $T_1 = 2\pi/\omega_1$ ) for the initial pulse and the parameters  $A_1 = 0.1058$  a.u. ( $I_1 = 3.9 \times 10^{14}$  W/cm<sup>2</sup>),  $A_2 =$

$0.0473$  a.u. ( $I_2 = 7.9 \times 10^{13}$  W/cm<sup>2</sup>),  $\phi = 0.558\pi$ , and  $\tau = 0.182T_1$  for the optimized pulse.

Figure 1(b) compares two HHG spectra generated by the initial unoptimized pulse [blue (dark gray) line] and by the optimized laser field [red (light gray) line]. It is found that the HHG plateau is significantly enhanced and extended by the optimized laser field [red (light gray) line]. Moreover, despite the fact that the total amplitude of the optimized field  $A_{\text{opt}}$  is only slightly larger than that of the initial field  $A_{\text{int}}$  (i.e.,  $A_{\text{opt}} \approx 1.1 A_{\text{int}}$ ), the optimized HHG has a much larger energy cutoff at the 850th order, compared to the unoptimized energy cutoff at the 750th order. In our optimal control trials, it was found that further increasing the peak amplitude of the optimized pulse leads to ionization of electrons and thus a fall in generation of HHG. This finding is in contrast to the common notion that a cutoff energy would increase as the amplitude of the laser field is increased as a result of the well-known expression [17] for the ponderomotive potential  $U_p \propto I\lambda^2$ , where  $I$  and  $\lambda$  are the intensity and wavelength of the laser field, respectively. However, this simple rule of thumb did not take into account the saturation effect of the ionization of the electron, which would prevent the intensity of a laser field from increasing indefinitely. Evidently, in addition to the amplitude, the CEP and time delay also play crucial roles in the improvement of the HHG.

The extension of the HHG plateau cutoff and the generation of the ultrashort attosecond pulse can be further understood by performing customary classical trajectory simulations and quantum time-frequency analysis. The results are presented in Figs. 2(a) and 2(b) for the initial and optimized pulses, respectively. It is unambiguously seen in the classical returning energy maps (thin yellow lines) that the maximum energy of the HHG plateau for the optimized pulse is located around the 850th order [Fig. 2(b)], while that of the initial one is located at around the 750 order [Fig. 2(a)], in agreement with the cutoffs of the HHG spectra shown in Fig. 1(b). Especially with the optimized pulse, it was found in Fig. 2(b) that the long-trajectory electrons, which give rise to a broad spectrum of harmonics from the 300th to the 600th order in the middle peak, return to the hydrogen ion nearly simultaneously and dominate the HHG. Not only do the optimized HHG spectra come predominately and simultaneously from one single quantum path corresponding to the long trajectories, but also the path contains a very broad (ultrabroad) supercontinuum spectrum, and it is very efficient to superpose the spectra and form a single attosecond pulse directly. In contrast, with the initial pulse, it is seen in Fig. 2(a) that the extent of harmonics associated with the long trajectories is much narrower, here from the 460th to the 607th order. As a result, fewer harmonics are available, thus making the generation of the desired ultrashort attosecond pulse less likely, even though the harmonics from 460th to the 750th harmonics also mainly come from one single quantum path belonging to the long trajectories. We note that short-trajectory electron emission with the optimized pulse also exists, as seen in Fig. 2(b), but the contribution of the long-trajectory electron emission is clearly much stronger.

Plotted in Fig. 3 are the attosecond pulses generated by the initial and optimized pulses. Figure 3(a) shows an isolated 47-as pulse created by superposing the harmonics from the 460th to the 607th orders generated by the initial laser pulse,

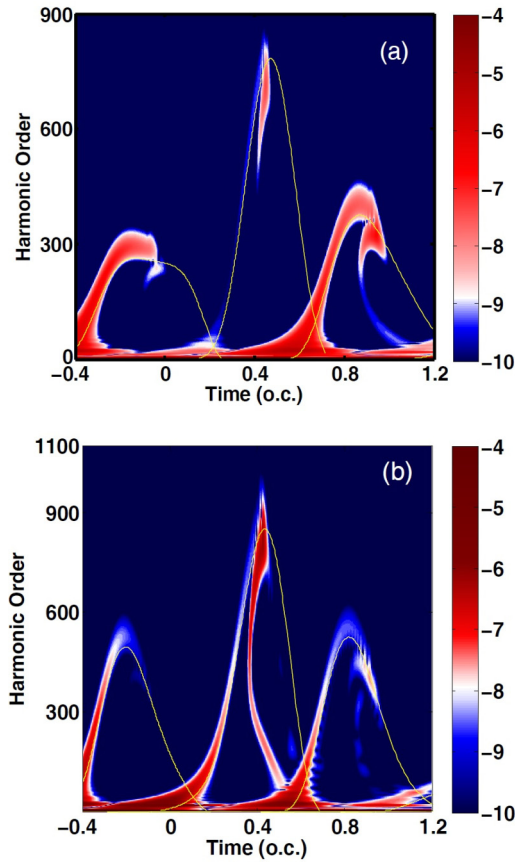


FIG. 2. (Color online) Wavelet time-frequency profiles of the HHG spectra and classical returning energy maps (yellow solid lines) of hydrogen atoms driven by (a) the initial field and (b) the optimized field.

and Fig. 3(b) contains a single 21-as pulse created by the harmonics from the 310th to the 605th orders generated by the optimized laser pulse. It was found that the intensity of the optimized attosecond pulse is almost two orders of magnitude larger than that of the unoptimized one. However, it should be noted that superposing harmonics higher than the 605th harmonic order does not further reduce the pulse duration of the generated attosecond pulse since, generally, both the short-trajectory electrons and the long-trajectory electrons contribute equally to the HHG near the cutoff in a homogeneous laser field. Moreover, to further understand the generation of the ultrabroad ultrashort pulse, we show in Fig. 4 the time profile of a sequence of the constituent harmonics of the 21-as pulse given in Fig. 3(b). It is seen that the peak of each harmonic profile originates from a long-trajectory electron as a result of the synchronization, which is a prerequisite of a dependable attosecond pulse. Finally, we note that the simulations here do not consider the macroscopic propagation effect associated with the transverse distribution of the intensity of the pump laser on the HHG in order to accommodate the well-known fact that the high-order-harmonic generation depends on both the single-atom response and macroscopic phase matching [18]. However, as pointed out in a previous work [19], despite the increasing contribution of the short-trajectory electron emission as a result of the macroscopic propagation, the characteristics of the optimized supercontinuum harmonics

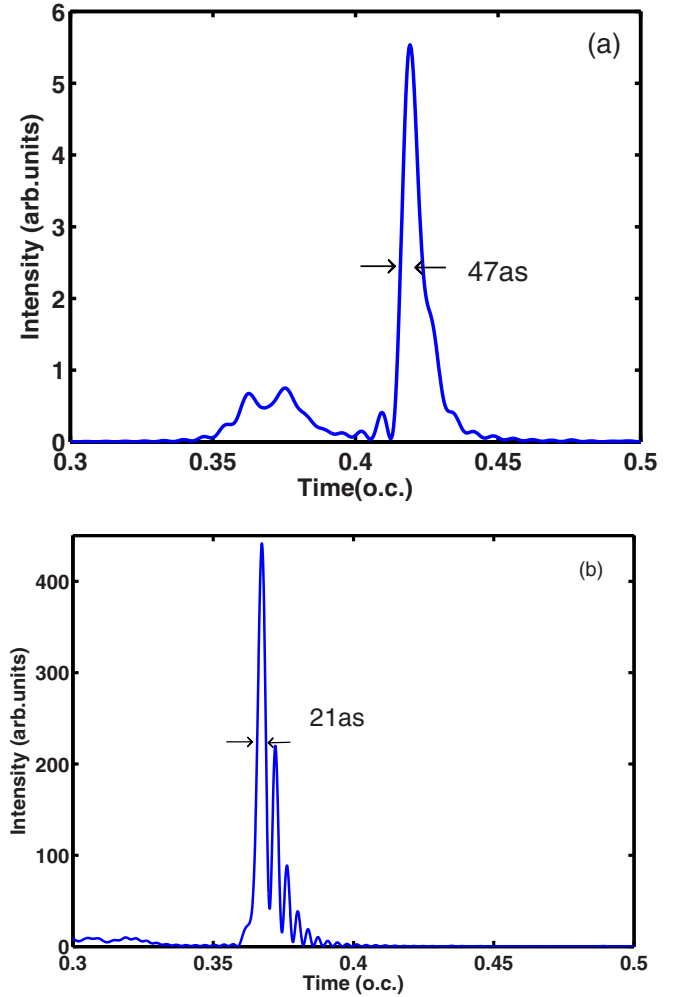


FIG. 3. (Color online) Attosecond pulses. (a) Initial laser field. (b) Optimized laser field.

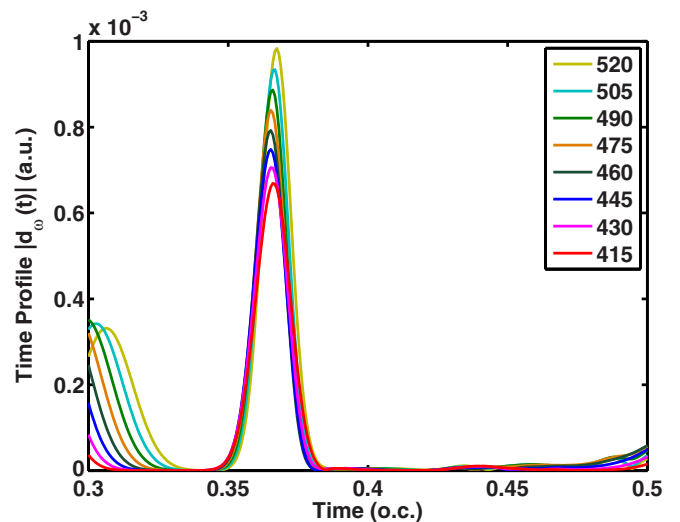


FIG. 4. (Color online) The corresponding time profile of the consecutive harmonics in generation of the 21-as pulse.

are still dominated by the long-trajectory electron emission for both on-axis and off-axis cases in the far field, which is similar to the findings of the current study without taking into account the effect of the transverse pump laser intensity. As a result, we expect that generation of a single ultrashort attosecond pulse subject to the transverse distribution of the pump laser intensity can still be realized using the same optimal control scheme proposed in this work.

## V. CONCLUSION

In summary, we have extended optimal control theory using a derivative-free optimization algorithm, NEWUOA, to produce a single ultrashort attosecond pulse for a hydrogen atom in a two-color laser field. Dealing with intense laser pulses, the TDGPS method provides us with an efficient and accurate way to solve the TDSE. Our results demonstrate that either the HHG is enhanced or the HHG plateau is extended with the optimized pulse. Furthermore, the optimized pulse

can result in a single ultrashort pulse that is not only much shorter but also more intense, by two orders of magnitude, than that produced by the initial one. The proposed method is expected to serve as a viable means in generating ultrashort attosecond pulses experimentally.

## ACKNOWLEDGMENTS

This work was partially supported by the Chemical Sciences, Geosciences, and Biosciences Division of the Office of Basic Energy Sciences, Office of Sciences, U.S. Department of Energy and by the U.S. National Science Foundation. We also would like to thank the Ministry of Science and Technology of Taiwan and National Taiwan University (Grants No. 104R8914 and No. 104R8700-2) for partial support. P.-C.L. is partially supported by the National Natural Science Foundation of China (Grants No. 11364039 and No. 11465016), the Natural Science Foundation of Gansu Province (Grant No. 1308RJZA195), and the Education Department of Gansu Province (Grant No. 2014A-010).

- 
- [1] F. Krausz and M. Ivanov, *Rev. Mod. Phys.* **81**, 163 (2009).
  - [2] J. J. Carrera, X. M. Tong, and Shih-I Chu, *Phys. Rev. A* **74**, 023404 (2006).
  - [3] K. Zhao, Q. Zhang, M. Chini, Y. Wu, X. Wang, and Z. Chang, *Opt. Lett.* **37**, 3891 (2012).
  - [4] P. B. Corkum, *Phys. Rev. Lett.* **71**, 1994 (1993).
  - [5] C. Brif, R. Chakrabarti, and H. Rabitz, *New J. Phys.* **12**, 075008 (2010).
  - [6] J. Werschnik and E. K. U. Gross, *J. Phys. B* **40**, R175 (2007).
  - [7] K. Krieger, A. Castro, and E. Gross, *Chem. Phys.* **391**, 50 (2011).
  - [8] A. Castro, E. Rsnen, A. Rubio, and E. K. U. Gross, *Europhys. Lett.* **87**, 53001 (2009).
  - [9] E. Räsänen and L. B. Madsen, *Phys. Rev. A* **86**, 033426 (2012).
  - [10] M. Hellgren, E. Räsänen, and E. K. U. Gross, *Phys. Rev. A* **88**, 013414 (2013).
  - [11] J. Xu, B. Zeng, and Y. Yu, *Phys. Rev. A* **82**, 053822 (2010).
  - [12] L. Feng and T. Chu, *Phys. Rev. A* **84**, 053853 (2011).
  - [13] P.-C. Li, C. Laughlin, and Shih-I Chu, *Phys. Rev. A* **89**, 023431 (2014).
  - [14] I.-L. Liu, P.-C. Li, and Shih-I Chu, *Phys. Rev. A* **84**, 033414 (2011).
  - [15] X.-M. Tong and S.-I. Chu, *Chem. Phys.* **217**, 119 (1997).
  - [16] M. Powell, in *Large-Scale Nonlinear Optimization*, edited by G. Di Pillo and M. Roma, Nonconvex Optimization and Its Applications Vol. 83 (Springer, New York, 2006), pp. 255–297.
  - [17] J. L. Krause, K. J. Schafer, and K. C. Kulander, *Phys. Rev. Lett.* **68**, 3535 (1992).
  - [18] M. B. Gaarde, J. L. Tate, and K. J. Schafer, *J. Phys. B* **41**, 132001 (2008).
  - [19] P.-C. Li and Shih-I Chu, *Phys. Rev. A* **86**, 013411 (2012).